Importance of Geosat orbit and tidal errors in the estimation of large-scale Indian Ocean variations

Altimetry
Orbit
Tide
Large scale
Indian Ocean

Altimétrie
Orbite
Marée
Grande échelle
Océan Indien

Claire PERIGAUD and Victor ZLOTNICKI

Jet Propulsion Laboratory, California Institute of Technology, MS 300/323, 4800 Oak Grove Drive, Pasadena, CA 91109, USA.

ABSTRACT

Geosat ERM data concerning the Indian Ocean over a period of 26 months were processed with two different techniques of orbit error reduction in order to improve the accuracy of estimates of large-scale meridional sea-level variations. The first technique removes an along-track polynomial of degree 1 over ~ 5,000 km; the second removes an along-track once-per-revolution sine wave (~ 40,000 km). Averaged over the Indian Ocean, the difference between the two estimates represents 43 % of the total variance and 31 % of the annual variance. This difference contains both oceanic and error signals. Sea-level variations from both techniques show an error with a spectral peak at 7°6 zonal wavelength, 317-day period, propagating westward at 2.6 km/day. This error is caused by the M2 tidal signal being inaccurately corrected and then aliased by Geosat's sampling characteristics into low-frequency apparent sea-level variations. We remove the tidal error by filtering out the spectral peak in the frequency-zonal wave number and re-analyze the estimated sea level. The polynomial technique produces stronger attenuation of both the tidal error and the large-scale oceanic signal. The annual variance retained by the filter contains 9 and 14 % of the respective annual variances of the two techniques before filtering. After filtering, the residual difference between the two methods represents 44 % of the total variance and 23 % of the annual variance. The sine-wave method yields a larger estimate of annual and interrannual meridional variations. Driven by the monsoon, the difference in sea level between the northern and southern basins (over 10°-20° S) decreases from May to November. This sea-level change is estimated at 19.6 cm and 15.6 cm by the two techniques. Similarly, in 1988 the sea level averaged from July to December is higher than in 1987 over the band from the equator to 10° N. This sea-level change is estimated at 3.0 and 1.0 cm by the two techniques.

Oceanologica Acta, 1992. **15**, 5, 491-505.

RÉSUMÉ

Importance des erreurs d'orbite et de marées dans Geosat pour l'estimation des variations à grande échelle de l'Océan Indien

Les données Geosat ERM ont été traitées sur l'Océan Indien avec deux techniques différentes de réduction d'erreur d'orbite dans le but d'améliorer la précision des variations grandes échelles méridionales. La première technique retire un polynome de degré 1 sur environ 5 000 km le long de chaque trace; la seconde retire une fonction sinus de 40 000 km le long de chaque arc ayant une révolution de longueur. En moyenne sur l'Océan Indien, la différence entre ces deux estimations contient 43 % de la variance totale et 31 % de la variance annuelle. Cette différence contient à la fois du signal océanique et des erreurs. De fait, les deux estimations contiennent une erreur qui apparaît dans l'analyse spectrale à 7,6° de distance zonale et 317 jours de période, se propageant vers l'Ouest à environ 2,6

km/jour. Cette erreur est due au signal résiduel de marée océanique M2 après correction ; ce signal est biaisé par Geosat en une variation basse-fréquence du niveau de la mer. Nous retirons cette erreur de marée en filtrant le pic d'énergie dans la bande de fréquences et de longueurs d'onde correspondantes et ré-analysons les variations du niveau de la mer. La technique polynomiale atténue à la fois l'erreur de marée et le signal océanique grande échelle. La variance annuelle retenue par le filtrage contient 9 et 14 % de la variance annuelle avant filtrage pour les deux techniques. Après filtrage, la différence résiduelle entre les deux techniques contient 44 % de la variance totale et 23 % de la variance annuelle. La technique sinusoïdale donne des variations méridiennes annuelles et interrannuelles plus fortes. Entraînée par la mousson, la différence de niveau de la mer entre les bassins nord et sud (entre 10° et 20° S) diminue de mai à novembre. Cette différence est estimée à 19,6 et 15,6 cm par les deux techniques. De même, le niveau moyen de la mer de juillet à décembre 1988 est plus haut que l'année précédente dans la bande qui s'étend de l'équateur à 10° N. Ce changement est estimé à 3,0 et 1,0 cm par les deux techniques.

Oceanologica Acta, 1992. **15**, 5, 491-505.

INTRODUCTION

Geosat furnishes a unique opportunity to study the low-frequency variability of the ocean. Up to now most of the results derived from Geosat have been obtained after removal of a polynomial (computed with an along-track least-square fit) in order to reduce the orbit error (*e. g.*, Zlotnicki *et al.*, 1989). For example, this is the case of the sea-level changes derived from Geosat over the tropical Pacific Ocean (Miller *et al.*, 1988) or over the tropical Atlantic Ocean (Arnault *et al.*, 1990). However, the large-scale oceanic variations are reduced in the process. The removal of an along-track sine function with a period equal to the satellite revolution over a complete revolution (*e. g.*, Tai, 1991) reduces the orbit error and, less significantly, the oceanic signal. For the first time, results derived from Geosat after removing such a sine function have recently been published (Cartwright and Ray, 1990). But the sinewave method also has drawbacks: it neglects all the long-wavelength errors which do not have the once-per-revolution frequency. Both methods thus have advantages and limitations.

The two methods have been applied to the Indian Ocean, which provides a good example for analyzing large-scale meridional sea-level variations. Due to the monsoon wind regime, the Somali current reverses each year. This implies mass and heat exchanges between the southern and northern parts of the Indian Ocean, exchanges which play a key role in the climate of the region. Few observations have, however, been available up to now to quantify these exchanges. Most of the observations cover the western and equatorial domain (for a review, *see e. g.* Schott, 1987). Very little data are available for the southern Indian Ocean. For seasonal variations of the dynamic height or mixed layer depth, the reader is referred to Wyrtki (1971) and Rao *et al.* (1989). Altimetric data can provide estimates of such variations. An important step is to determine their accuracy.

Different Geosat analyses have been performed over the Indian Ocean, concerning which a shallow-water model has been run to simulate wind-driven sea level variations (Périgaud and Delécluse, 1989). Annual sea-level variations from Geosat ERM data obtained with the polynomial method show good agreement with the simulations driven by observed contemporary winds (Périgaud and Delécluse, 1991 *a* ; 1992). In particular, the observed and simulated meridional large-scale variations have similar amplitudes. However, such altimetric variations may have a reduced amplitude compared with the actual oceanic ones because the method of orbit error reduction reduces any long-wavelength meridional signal. Similarly, the simulated large-scale meridional variations may be smaller than the actual ones. Indeed, such variations are very difficult to simulate accurately: experiments with the shallow-water model have demonstrated their high sensitivity to initial conditions and to wind errors. Apart form these error sources in the simulations, thermodynamic forcing is not taken into account in the shallow-water model, whereas it plays an important role in the Indian Ocean. Comparison between the results obtained by the two different methods of orbit error reduction thus constitutes a determinant step in the quantification and understanding of the meridional large-scale variations of the Indian Ocean. Furthermore the present study was motivated by the unexpected finding that the source of discrepancy due to difference in the orbit error reduction method is by far the largest among the different error sources analyzed (Périgaud and Zlotnicki, 1992): it is much greater than the discrepancy due to tropospheric uncertainty as estimated with FNOC (Cheney *et al.*, 1987) or SSMI corrections (Wentz, 1988) and larger than the discrepancy due to orbit model as estimated with NAG (Cheney *et al.*, 1987) or GEMT2 (Haines *et al.*, 1990).

This paper is based on results derived from processing that was identical except for the orbit error reduction method. This is briefly described in the next section. In the third section, results are statistically examined for both approaches,

with particular reference to the space-time characteristics of the differences. On the basis of these results, evidence of the presence of the aliased M2-tidal error is provided in the fourth section. In the fifth section filtering is proposed to separate this error from the oceanic variations. The error content of the filtered results is discussed in the sixth and seventh sections. The oceanic signal is statistically examined in the eighth one. Lastly, the impact of both techniques for large-scale oceanic variations is discussed.

ALTIMETER DATA PROCESSING

Initial processing of ERM Geosat GDR has been applied for editing and along-track gridding as explained in Zlotnicki *et al.* (1990). Traditional corrections have been applied as explained *in* Périgaud (1990), except for tropospheric corrections which are SSMI corrections (Wentz, 1988) after, and FNOC corrections before, July 1987. The same space-time analysis based on a successive correction scheme has been applied over the Indian Ocean with the same parameters as in Périgaud and Delécluse (1991): results cover the domain 30° S-23° N, 30°-115° E from 15 November 1986 to 5 January 1989 with a resolution of one degree of latitude and longitude and ten days in time.

This paper is focused on differences in the results derived from two different methods of orbit error reduction. The polynomial method as performed in Zlotnicki (1991), consists in retrieving a tilt and bias along each repeat track of the different satellite passes limited by boundaries as shown on Figure 1. The second method involves retrieving an along-track sine function with a wavelength equal to the Earth's circumference, each arc having a length equal to one revolution (*see* Appendix). The results are hereafter referred to as "D1" for the polynomial method (to remember that a "Degree 1" has been removed) and "SW" for the second one (to remember that a "Sine Wave" has been removed).

Large-scale meridional oceanic variations are preserved by the SW method. However, this method ignores any long-wavelength signal which does not have the specific period which is subtracted. In particular, the errors on the tidal correction are not reduced in SW as in D1. Thus the difference between the D1 and the SW results contains oceanic as well as residual orbit error and other error signals.

RESULTS OBTAINED FROM THE SW AND D1 METHODS

Variability maps derived from ten-day sea-level series over 26 months have been computed for the D1 and SW results (Fig. 2, top). D1 maps contain the "zero order" picture of ocean variability as described and compared with simulations in Périgaud and Delécluse (1991 *a* and 1992). The equatorial wave guide presents a low variability whereas maxima are found along the boundaries of the Arabian Sea and of the Bay of Bengal (Somali current and currents along the coast of India) and in the 10° S-20° S zonal band (along the South Equatorial Current). Averaged over the whole oceanic domain, the variability is higher for SW than for D1 (9.1 and 8.1 cm respectively). The annual cycle accounts for 19 and 17 % respectively of the total variance (Fig. 2, bottom). The patterns of strong annual variations in the southern part of the domain have a zonally-oriented preferred direction. As explained in Périgaud and Delécluse (1991 *b*),

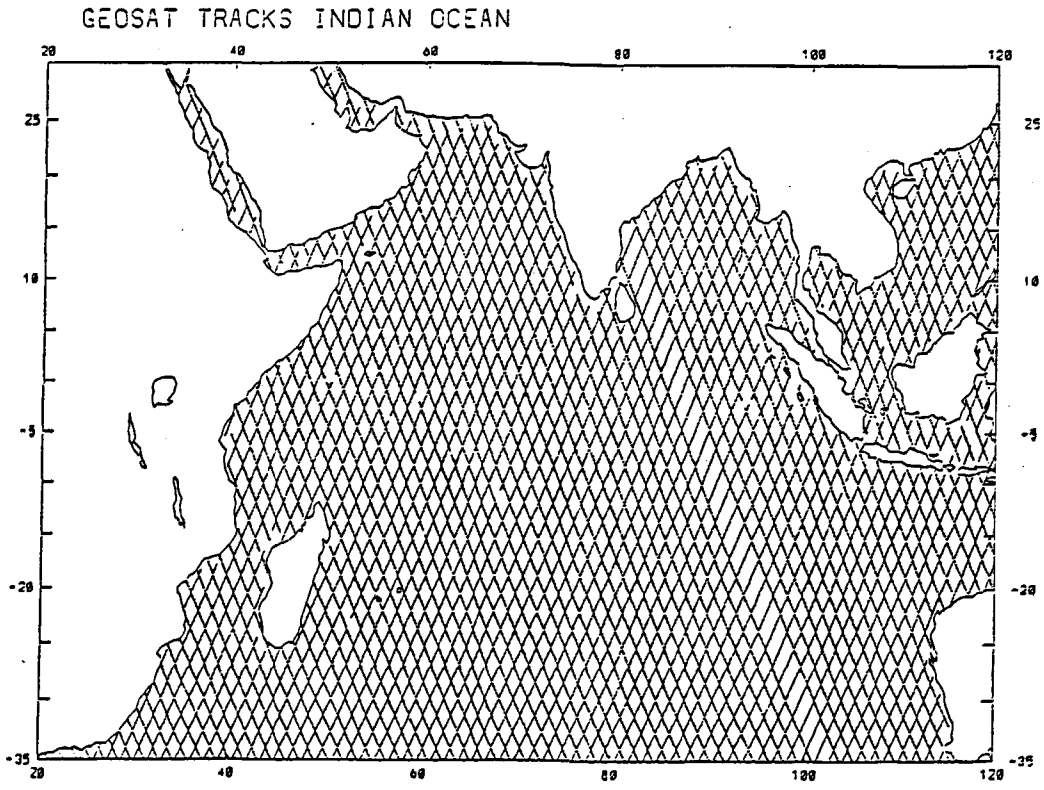

Figure 1

Domain over which the D1 method was applied with the coverage of Geosat given for cycle 22.

Domaine d'application de la méthode «D1» avec couverture de Geosat pour le cycle 22.

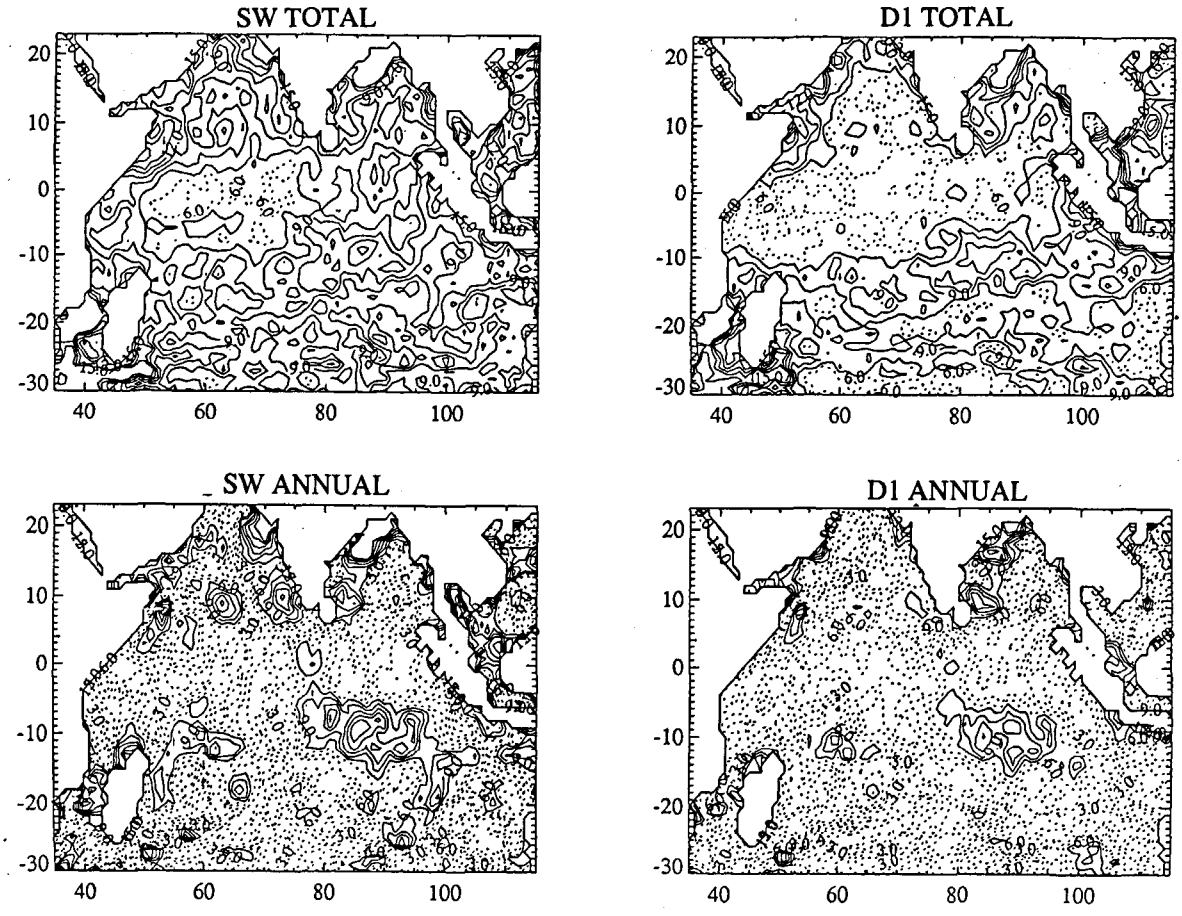

Figure 2

RMS variability (top) and annual amplitude (bottom) of sea-level series derived from SW method or D1 method. Isocontours are 1.5 cm with dotted lines for amplitude smaller than 6.0 cm, plain lines above 7.5 cm.

Variabilité RMS (haut) et amplitude annuelle (bas) du niveau de la mer déduit de la méthode «SW» ou «D1». Les isocontours sont de 1,5 cm. Les lignes en pointillés correspondent à des valeurs inférieures à 6 cm, les lignes pleines à des valeurs supérieures à 7,5 cm.

this corresponds to long Rossby waves generated by the monsoon wind reversal over the eastern domain which radiate away from the eastern boundary and propagate across the entire basin in a west-southwestward direction.

Maps (every ten days) of sea-level variations from both D1 and SW results were differentiated at corresponding times. The rms variability of the differences is presented for the ten-day series and for its annual cycle component only (Fig. 3). The largest differences are found all along the continental boundaries of our domain but the difference is in fact also large far offshore throughout the domain. The variance of the total difference is 43 % of the mean variance of the signals derived from SW and D1 (Tab. 2). Note that these estimates depend on the domain over which they are averaged: total variance is larger close to the boundaries than offshore. For this reason, all statistics in Tables 1 and 2 are given for two different domains, the entire oceanic domain or the offshore domain (60°-100° E, 30° S-5° N). For simplicity and unless specified, the statistics given in the text refer to the whole domain. The variance of the difference at the annual period is 31 % of its mean annual variance. This difference *a priori* contains both ocean and error signals. The reader can readily identify the presence of error as the patterns of this map (Fig. 3, top) have a preferred orientation aligned with the satellite tracks. This is even more visible on the annual cycle. The "trackiness" pattern is particularly well pronounced with a zonal wavelength of the order of 8° of longitude. This wavelength is larger than the distance between crossovers (order of 1°5). Similarly, the along-track distance between maxima is larger than the crosstrack distance. So this error is not directly due to the satellite sampling, but results from a large-scale signal which is aliased by the satellite as demonstrated below.

EVIDENCE OF THE PRESENCE OF ERROR DUE TO THE M2-TIDAL SIGNAL

The presence of such an error is further evidenced along zonal sections of the difference between SW and D1 (Fig. 4 *a*, *b*, *c*): the 8° patterns are propagating westward with a speed of the order of 2.5 km/day. This zonal propagation is found on all sections independently of latitude, and is particularly well identified in the annual cycle. In the tropical 40° band, this does not correspond to oceanic variations such as long Rossby waves which were found in good

agreement with simulations derived from the shallow-water model. Those waves have a faster westward speed which decreases with increasing distance from the equator - of the order of 80 km/day along the equator, 18 km/day along 10° S and 5 km/day along 20° S.

Table 1

Total and annual variance (in cm^2) of SW, D1 and SW-D1 averaged over the total oceanic domain (35°-115° E, 30°S-23° N) or over the interior ocean (60°-100° E, 30° S-5° N). Values in percents indicate variance contained in filtered and residual results relative to unfiltered results.

Variance totale et annuelle (en cm^2) de «SW», «D1», «SW-D1», moyennée sur le domaine océanique total ou restreint à 60°E-100°E, 30°S-5°N. Les valeurs en pourcentages indiquent la variance contenue dans les résultats filtrés et résiduels par rapport à la variance des résultats non filtrés.

	TOTAL		ANNUAL	
	Global	**Interior**	**Global**	**Interior**
$\langle \lvert SW \rvert^2 \rangle$	96	74	19	15
$\frac{\langle \lvert SWFILT \rvert^2 \rangle}{\langle \lvert SW \rvert^2 \rangle}$	5 %	4 %	14 %	13 %
$\frac{\langle \lvert SWR \rvert^2 \rangle}{\langle \lvert SW \rvert^2 \rangle}$	94 %	100 %	80 %	89 %
$\langle \lvert D1 \rvert^2 \rangle$	66	51	11	10
$\langle \lvert D1FILT \rvert^2 \rangle / \langle \lvert D1 \rvert^2 \rangle$	3 %	1 %	9 %	6 %
$\lvert D1R \rvert^2 \rangle / \langle \lvert D1 \rvert^2 \rangle$	92 %	97 %	84 %	96%
$\frac{\langle \lvert SW\text{-}D1 \rvert^2 \rangle}{\langle \lvert SWFILT\text{-}D1FILT \rvert^2 \rangle}$	35	13	5	2
$\frac{\langle \lvert SW\text{-}D1 \rvert^2 \rangle}{\langle \lvert SWR\text{-}D1R \rvert^2 \rangle}$	7 %	12 %	30 %	45 %
$\frac{\langle \lvert SW\text{-}D1 \rvert^2 \rangle}{\langle \lvert SW \rvert^2 \rangle}$	90 %	89 %	64 %	62 %

Table 2

Mean variance in cm^2 contained in SW and D1 before filtering, in the filtered SWFILT and D1FILT, or in the residual SWR and D1R after filtering. Variance contained in their difference (SW-D1), (SWFILT-D1FILT), (SWR-D1R) and ratio of this difference to the respective mean variance.

Variance moyenne (en cm^2) contenue dans «SW» et «D1» avant filtrage, dans «SWFILT» et «D1FILT», ou dans les résidus «SWR» et «D1» après filtrage, variance contenue dans leur différence (SW-D1), (SWFILT-D1FILT), (SWR-D1R) et rapport de cette différence sur la variance moyenne respective.

	TOTAL		ANNUAL	
	Global	**Interior**	**Global**	**Interior**
$\sqrt{\langle \lvert SW \rvert^2 \rangle \langle \lvert D1 \rvert^2 \rangle}$	80	61	17	12
$\langle \lvert SW\text{-}D1 \rvert^2 \rangle$	35	13	5	2
$\frac{\langle \lvert SW\text{-}D1 \rvert^2 \rangle}{\sqrt{\langle \lvert SW \rvert^2 \rangle \langle \lvert D1 \rvert^2 \rangle}}$	43 %	22 %	31 %	16 %
$\sqrt{\langle \lvert SWF \rvert^2 \rangle \langle \lvert D1F \rvert^2 \rangle}$	3.9	1.7	2.5	1.4
$\langle \lvert SWF\text{-}D1F \rvert^2 \rangle$	3.4	1.4	2.0	1.3
$\frac{\langle \lvert SWF\text{-}D1F \rvert^2 \rangle}{\sqrt{\langle \lvert SWF \rvert^2 \rangle \langle \lvert D1F \rvert^2 \rangle}}$	88 %	85 %	80 %	92 %
$\sqrt{\langle \lvert SWR \rvert^2 \rangle \langle \lvert D1R \rvert^2 \rangle}$	73	62	12	11
$\langle \lvert SWR\text{-}D1R \rvert^2 \rangle$	31	12	3	2
$\frac{\langle \lvert SWR\text{-}D1R \rvert^2 \rangle}{\sqrt{\langle \lvert SWR \rvert^2 \rangle \langle \lvert D1R \rvert^2 \rangle}}$	44 %	20 %	23 %	14 %

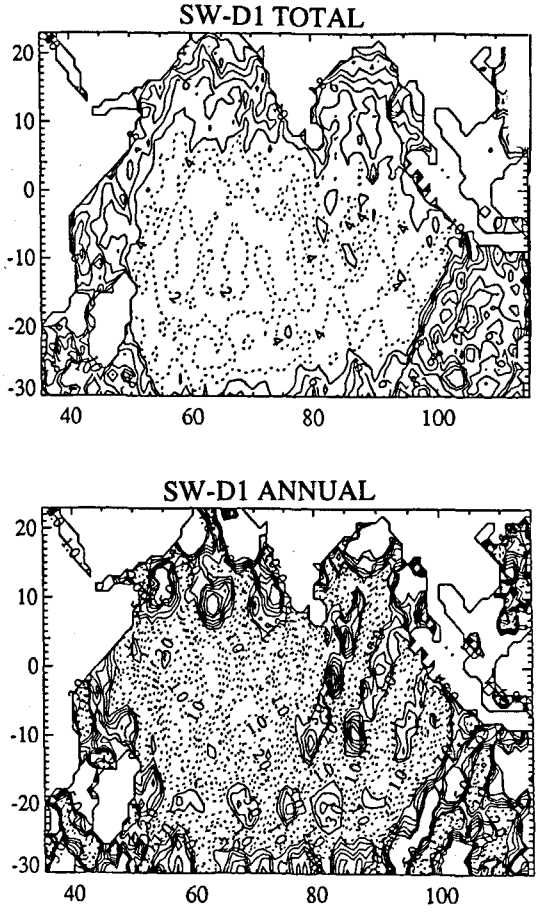

Figure 3

RMS variability (top) and annual amplitude (bottom) of the sea-level differences between SW and D1 variations. Isocontours on top are 1 cm (top) and 0.5 cm (bottom) with dotted lines below 4 cm (top) or 2 cm (bottom), plain lines above 5 cm (top) or 2.5 cm (bottom).

Variabilité RMS (haut) et amplitude annuelle (bas) des différences entre les variations «D1» et «SW». Les isocontours sont de 1 cm (haut) ou 0,5 cm (bas). Les lignes en pointillés correspondent à des valeurs inférieures à 4 cm (haut) ou à 2 cm (bas).

This error is due to M2-tides which are aliased by the satellite's peculiar sampling (*see* also Jacobs *et al.*, 1991; Cartwright and Ray, 1990). The particular period of the error, 317 days, is simply the alias period of the M2 tide, T_{M2} = 12.420583 hours, when sampled every 17.0505 days, the repeat cycle of Geosat. The characteristic zonal wavelength of the error is also easy to understand given Geosat's sampling characteristics: for a given altimetric pass (1) crossing the equator, the altimetric pass (2) which is parallel to the given pass, spatially closest and to its east differs in equatorial crossing longitude Λ by Λ_2-Λ_1 = 1.475°, and is sampled t_2-t_1 = 3.005 days after the given pass. Assuming that the tidal amplitude and phase are constant over the 1.475°, then the M2 tide has gone through 5.806 cycles (= 3.005 * 24/12.420583) between the times t_1 and t_2. That implies a phase difference of ϕ_2-ϕ_1 = 1/5.168 cycles of M2 between two passes separated by Λ_2-Λ_1 = 1.475°. If the assumption of constant tidal coefficients can be extended (as a zeroth order approximation) over larger distances then a phase difference of one cycle of M2 corresponds to a longitude difference of 7.6°

Figure 4

Zonal sections as a function of longitude and time.

a, b, c: *Difference between SW and D1 sea-level variations.* a *and* b *are for the annual cycle.* c *is for the 10-day series. Isocontour is 1 cm with plain lines positive or nul, dotted lines negative.*

d: *Zonal section of the simulated aliased M2-tidal signal (normalized amplitude).*

e, f, g, h: *Annual sea-level variations for SW or "D1". Isocontour is 2 cm with plain lines positive or nul, dotted lines negative.*

Sections zonales en fonction de la longitude et du temps.

a, b, c : différence entre «SW» et «D1». *a* et *b* sont pour le cycle annuel ; *c* pour les séries à dix jours. L'isocontour est de 1 cm, les courbes pleines représentant les valeurs positives ou nulles.

d : section zonale du signal de marée M2 biaisé (amplitude normalisée).

e, f, g, h : variations annuelles pour «SW» et «D1». L'isocontour est de 2 cm, les courbes pleines représentant les valeurs positives ou nulles.

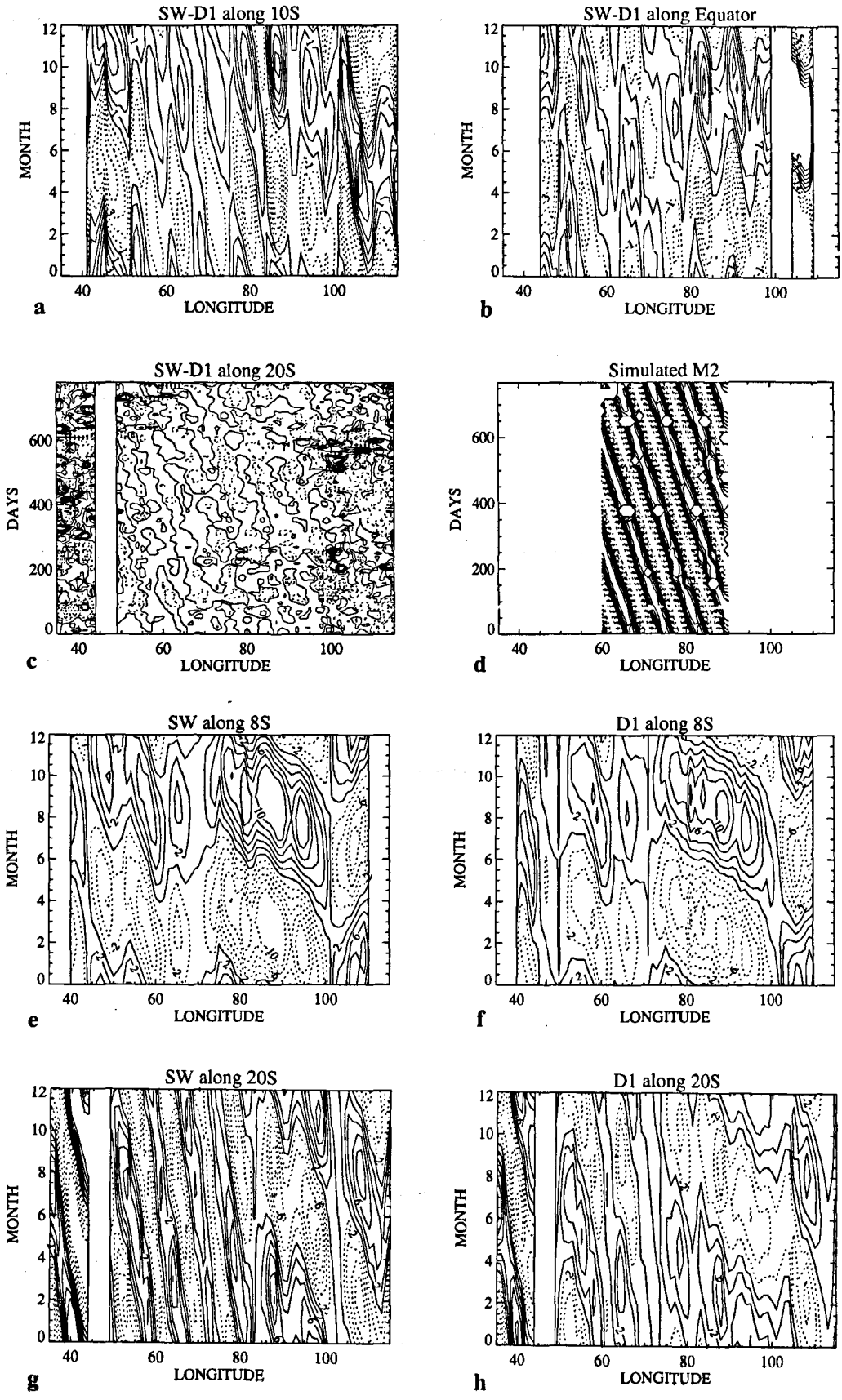

(= 1.475 * 5.168), which is approximately the observed characteristic zonal scale of the M2 error.

To obtain further proof that the error is indeed a tidal signal, we simulated such a signal between 60° E and 90° E along 20° S as follows:

Let the tidal signal "h_{tid}"' be of fixed amplitude and phase whatever the longitude x. Its value at time t is:

$h_{tid}(x, t) = \sin(2 * pi * t/T_{M2})$ with T_{M2} =12.420583 hours.

This signal was sampled at the times tg (x) which are those in the Geosat GDR from 8 November 1986 over 44 satellite

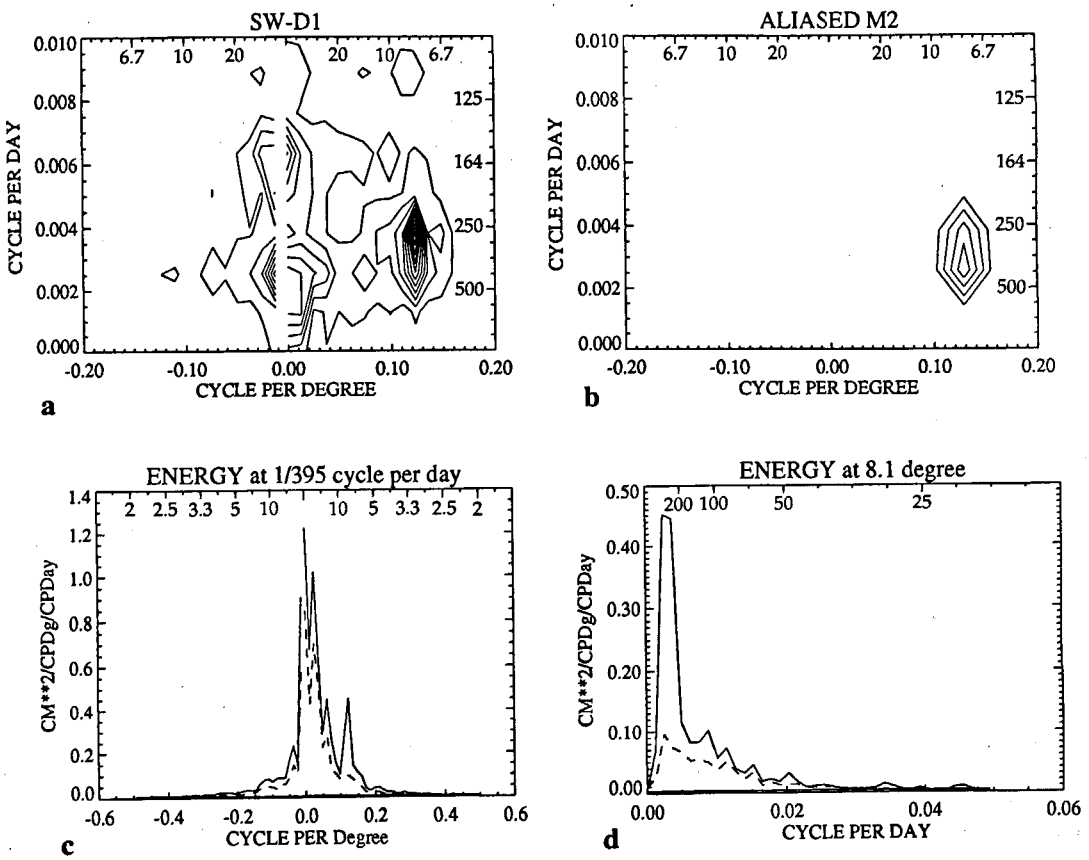

Figure 5

Wavenumber-frequency spectrum of SW-D1 (5 a) and aliased M2 signal (5 b). Wavenumber-frequency energy of SW (plain) or D1 (dashed) as a function of wavenumber at the frequency 1/395 days (5 c) and as a function of frequency at the wavelength 1/8.1° (5 d). Positive wavelength corresponds to propagation to the West.

Spectre en nombre d'onde et fréquence de «SW-D1» (a) et du signalM2 biaisé (b). Énergie à la période 395 jours en fonction du nombre d'onde (c) et énergie à la longueur d'onde 1/8,1° en fonction de la fréquence (d). Pour (c) et (d), la courbe pleine (en pointillés) correspond à «SW» («D1»).

cycles. In each 1° * 1° box the aliased signal is obtained by averaging h_{tid} [x, tg (x)] over each cycle, boxes without data being flagged. The aliased signal presents the 8° pattern which propagates westward at 2.5 km/day (Fig. 4 *d*). Indeed, Jacobs *et al.* (1991) have recently shown the presence of such an error in the annual cycle derived from Geosat.

Frequency-wavenumber spectra of the difference between D1 and SW were computed for each zonal section, using FFT after applying a Hanning window over the (80° * 790 days) domain. The average spectrum (Fig. 5 *a*) presents a peak at 8°.1 and 395 days, which corresponds to a 2.5 km/day westward propagation. Computed over the 60°-90° E and the 44 cycles of 17.0505 days, the frequency-wavenumber spectrum of the M2 aliased signal (Fig. 5 *b*) presents a peak at 7.5° and 375 days (these figures depend on the time and length span of the analyzed signals), and should be compared with the theoretical values of 317.388 days and 7.6° derived in the previous paragraph. Furthermore, M2 contaminates the annual cycle to such an extent because the total length of the time series, two years, defines a fundamental unit of frequency, 0.5 cy/yr, so that two spectral peaks in the data separated by less than 0.5 cy/yr cannot be resolved. Indeed, 1 - 365/317 = 0.15 < 0.5 cycles per year, the fundamental frequency of the time series. The D1 signal is also contaminated by this error (Fig. 4 *f* and 4 *h*): this error (visible on the western side of these sections) propagates faster than oceanic variations (visible on their eastern side). As explained in the first section, the D1 method reduces this error more than the SW method, which explains why SW (Fig. 4 *e* and 4 *g*) is more contaminated. It is thus crucial to retrieve this error before analyzing low-frequency variations from Geosat.

FILTERING

Cartwright and Ray (1990) estimated several tidal species by combining spatially neighbouring data assuming constant tides in the neighbourhood; Cartwright *et al.* (1991) used spherical harmonics as the spatial function, as Mazzega (1985) had done; Jacobs *et al.* (1991) retrieved the M2 error by combining the aliased coefficients of neighboring parallel tracks with their appropriate phase difference. Because these excellent methods are very demanding in computing power we chose a simpler but less accurate approach to remove the M2 error. We first need to explain why:

The 1°*1°*10 day analyses over the Indian Ocean constitute the basis of our data because their results have been analyzed and compared to numerical simulations - in case of a D1 reduction method. Our objectives here are:

- to show that the SW method contains an M2 error larger than the D1 method and estimate how much larger;
- to show that the SW method nevertheless retrieves large scale oceanic signals better than the D1 method; and to estimate how much better.

For these purposes the authors tested different simple means of retrieving the tidal error from the SW and D1 analyzed data sets. None proved fully satisfactory. Because of the proximity of the aliased period with the annual one, a filtering in time only over the 26 months of data is not possible. A filtering in both time and space is *a priori* much more efficient in sorting out the error from the oceanic signal as the (8°, 2.5 km/day) domain does not have much energy in the tropical oceans as in mid-latitudes. However, results still contain error. This is because the wavelength-frequency contaminated by the error is, for several reasons, not unique, one reason is that the M2 tide does not have a constant amplitude or phase over the whole domain. Another is that there is some energy left when filtering a finite series where gaps have been filled in with zeros. Yet another reason is that scales other than 7.6° may be contaminated by additional tidal components. Moreover, the filtering is performed after the space-time analysis and not directly on the along-track altimetric residuals. In particular, the space-time analysis involves successive correlation length scales varying from 4° to 1° and a time correlation scale of 10 days. Nonetheless this error has a pretty sharp peak in the wavenumber-frequency domain (Fig. 5 *c*, *d*) and this has driven the following choice.

We simply performed a zonal wavenumber-frequency decomposition of the 1°*1°*10 day analyses over the Indian Ocean, using a two-dimensional Fast Fourier Transform algorithm. We then set to zero the coefficients in the band t (1/395 to 1/263 days, 1/10.1° to 1/6.8°), and regenerated the time series by inverse Fourier transform. The bandwidth of this filter partly accomodates the variations of amplitude and phase of the tidal error over the domain. The authors are aware that this is not the best means of separating the oceanic signal from the tidal error, but it is a reasonable choice for their objectives. Below we give the results derived either from the band-pass filter (named "SWFILT" and "D1FILT") or from the residual part (named "SWR" and "D1R"). Tables 1 and 2 present the statistics derived from the different estimates, either averaged over the whole domain or averaged in the region (60°-100° E, 30° S-5° N) to keep away from boundary effects. Unless specified, the statistics given in the text refer to the whole domain.

RESULTS FROM THE BAND-PASS FILTER

Filtered results for the SW data ("SWFILT") contain 5 % of the SW total variance; "D1FILT" contain 3 % of the D1 total variance (Tab. 1). As expected D1FILT has a relatively lower variability than "SWFILT". This is because both fields contain the same mesoscale oceanic variability, as small-scale signals are not much affected by the orbit error

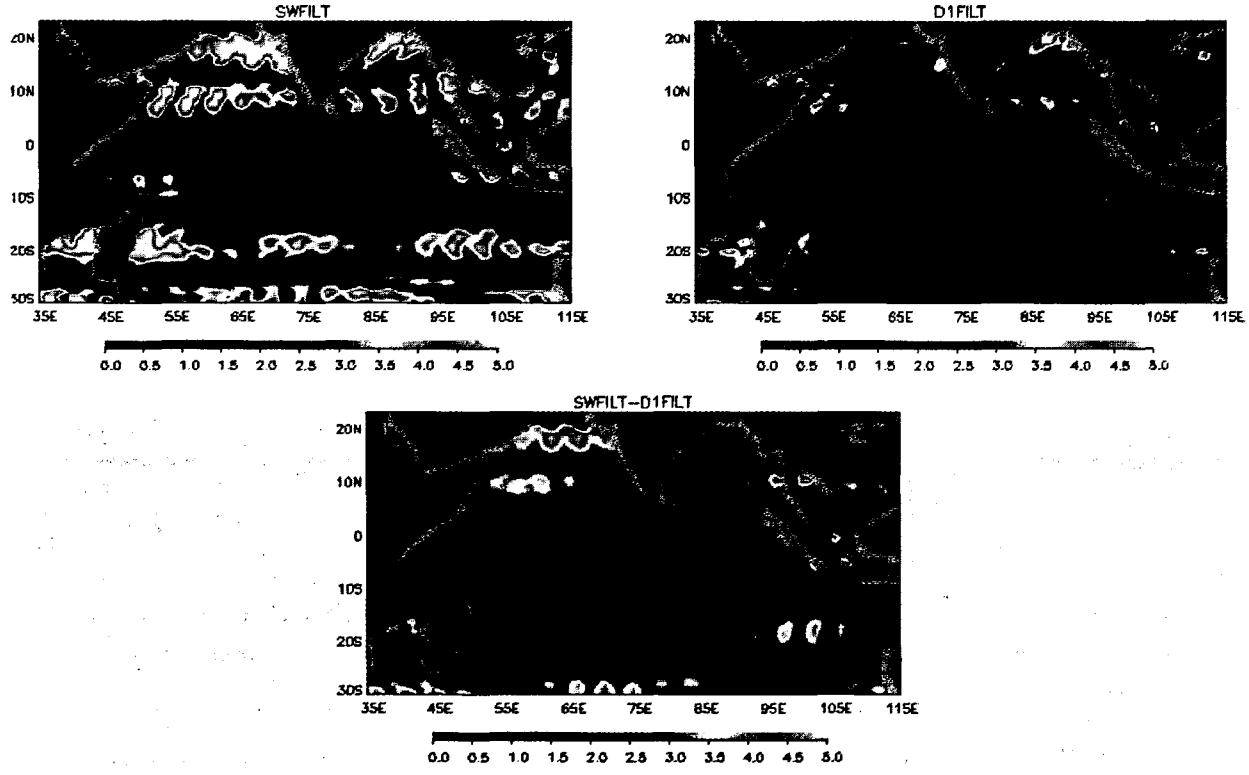

Figure 6

Annual amplitude of sea-level series contained in the filter SWFILT or D1FILT (top) and of their difference (bottom).

Amplitude annuelle du niveau de la mer contenu dans le filtre «SWFILT» ou «D1FILT» (haut) et dans leur différence (bas). Mêmes isocontours que sur la figure 3 (bas).

reduction process whereas tidal error is less reduced by the SW method. Of course this difference is more significant on the annual cycle: the variance contained in the filtered results amounts to 14 and 9 % for SWFILT and D1FILT respectively (Tab. 1). Sensitivity of the results to the band-pass has been analyzed with different filters. The percentage of total variance contained in the filtered results is, of course, sensitive to the band size as it contains more or less oceanic variance. The band chosen in this paper is that which maximizes the ratio of the SWFILT-D1FILT variance (mostly comprising error) over the D1FILT variance (which is the field containing relatively the most ocean signal). For all the filters tested, the map of SWFILT annual amplitude presents similar characteristics (Fig. 6, top): a minimum of variability in the 20° tropical band and four zones of strong amplitude outside this central zone; maxima are located along the northern border of Arabian Sea and the Bay of Bengal, in the Arabian Sea along 10° N (4 cm averaged annual amplitude between 55° and 65° E), and all across the basin to the south along 18° S (4 cm averaged from 55° to 105° E) and 28° S (3 cm averaged from 55° to 105° E). This spatial distribution of the tidal error was not expected and is difficult to interpret. Nonetheless and despite the crudeness of the filter, this has been found similar to results derived from

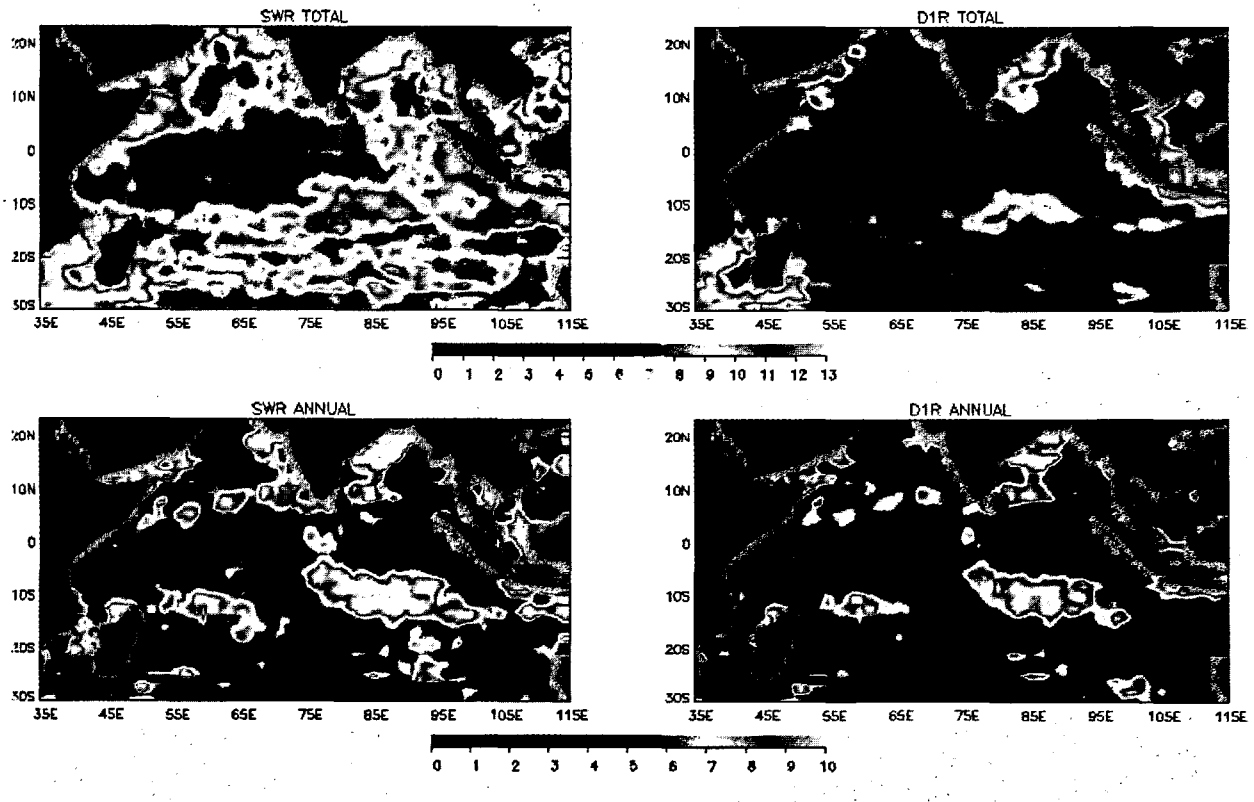

Figure 7

RMS variability of the 10-day (top) and annual amplitude (bottom) of sea- level series derived from SWR or D1R.

Variabilité RMS à dix jours (haut) et amplitude annuelle (bas) des séries déduites de «SWR» et «D1R». Mêmes isocontours que sur la figure 2.

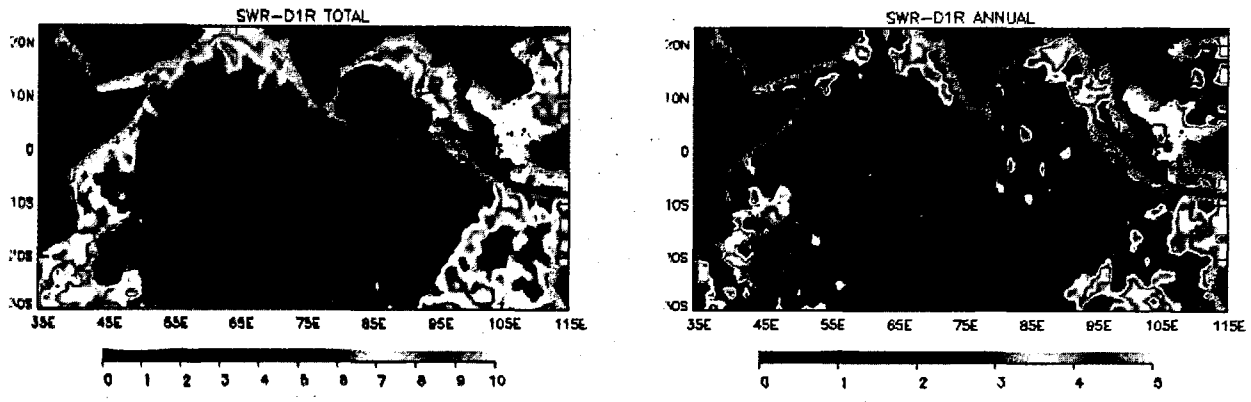

Figure 8

RMS variability (top) and annual amplitude (bottom) of the differences between SWR and D1R variations.

Variabilité RMS (haut) et amplitude annuelle (bas) des différences entre «SWR» et «D1R». Mêmes isocontours que sur la figure 3(haut).

two different and more efficient filters (Zlotnicki, 1992, pers. comm.; Fu and Vazquez, 1992, pers. comm.).

SWFILT and D1FILT were differentiated and their variability and annual cycle computed. The map of annual amplitude is presented on Figure 6 (bottom). This difference contains only error as the SW and D1 reduction process does not affect the band of wavenumber-frequency which has been passed. This difference represents the loss in accuracy of the SW method *versus* the D1 method, which is due to a less efficient reduction of the tidal error. Relative to the variance of the difference before filtering, this loss represents 7 % for the total variance and 30 % for the annual variance (Tab. 2). The remaining variance may be hopefully expected to contain the oceanic signal which has been gained by SW method relative to "D1". This is examined in the seventh and eighth sections.

RESULTS LEFT AFTER FILTERING

Maps of the variability left after filtering (SWR and D1R) are presented in Figure 7. Relative to the variance before filtering, SWR and D1R contain respectively 94 and 92 % of the total variance and 80 and 84 % of the annual variance (Tab. 1). Note that the sum of the filtered and residual variances is different from 100 % as those two fields are correlated in time. This is due to the amount of energy lost by the filtering process after filling in the continental domain with zeros. Maximum correlation for all estimates is 7 %. The "zeroth order" description which was given in the third section is now clearer. In addition these maps are strikingly different from the SWFILT and D1FILT presented above. The 20°-30° S band and the northern Arabian Sea now present a minimum of variability. The band centered along the South Equatorial Current (approximately 10° S) is now a zone of maximum variability. This contrast is fortunate: the areas with strong oceanic variations are contaminated by the tidal error to a lesser extent than the rest of the ocean. This is not the case, however, in the Bay of Bengal.

The SWR and D1R fields were differentiated; their variability maps are presented on Figure 8. Relative to the mean variance of the SWR and "D1R", this difference contains 44 % of the total variance and 23 % for the annual cycle (Tab. 2). The differences between SWR and D1R are mostly due either to edge effect as seen along the continental boundaries or to long along-track signal as seen in the central part of the domain. For both categories, SWR is expected to give a better estimate of the oceanic variations. In addition to not reducing the large-scale along-track signal as explained in the second section, the SWR is expected to correct more properly orbit errors close to the continental boundaries, as the removal of a sine function over a one-revolution arc is not as badly constrained as the removal of a degree 1 polynom with limits defined by continents. Such errors induced by edge effect in the polynomial removal have already been described (Sandwell and Zhang, 1989). However, in the present study the authors keep in mind that the removal of the tidal error is also poorly constrained close to the continents where results may be suspect. Indeed, when averaged over the domain from 30° S to 5° N and from 60° to 100° E only instead of over the whole basin, the percentage of annual variance contained in this difference is 14 % instead of 23 %. This SWR-D1R difference reflects the gain in accuracy of method SW *versus* D1 due to a better preservation of the along-track large-scale oceanic signal. In the following section we examine the significance of the signal contained in this difference.

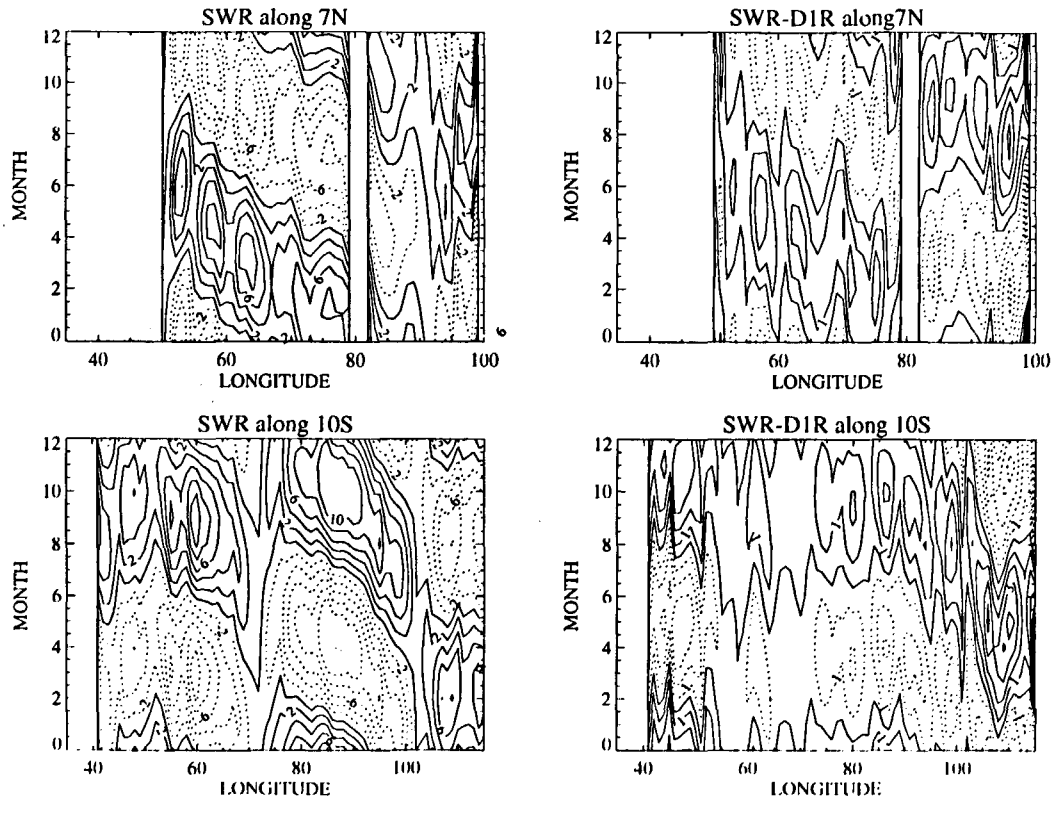

Figure 9

Zonal sections as a function of longitude and time of annual sea level variations from SWR and D1R. Same isocontour as Figures 4 e, f, g, h.

Sections zonales en fonction de la longitude et du temps des variations annuelles déduites de «SWR» et «D1R». Mêmes isocontours que sur la figure 4 *e, f, g, h.*

OCEANIC SIGNAL GAINED BY SWR *VERSUS* D1R

Annual and interranual variations may usefully serve to demonstrate the superiority of SWR *versus* D1R results when observing large-scale oceanic signals.

Annual variations have propagation characteristics which are well identified on zonal and meridional sections (Fig. 9 and 10). The westward and poleward propagation present in the SWR signal (and also present in the shallow-water simulations) is characteristic of the free Rossby waves (Schopf *et al.*, 1981) which in the Indian Ocean are generated each year by the monsoon wind reversal (Périgaud and Delécluse, 1991 *b*). The gain corresponds to an amplification of the variations as the correlation between SWR and SWR-D1R is positive (0.57). This can be explained as follows: variations of the northern basins are in opposite

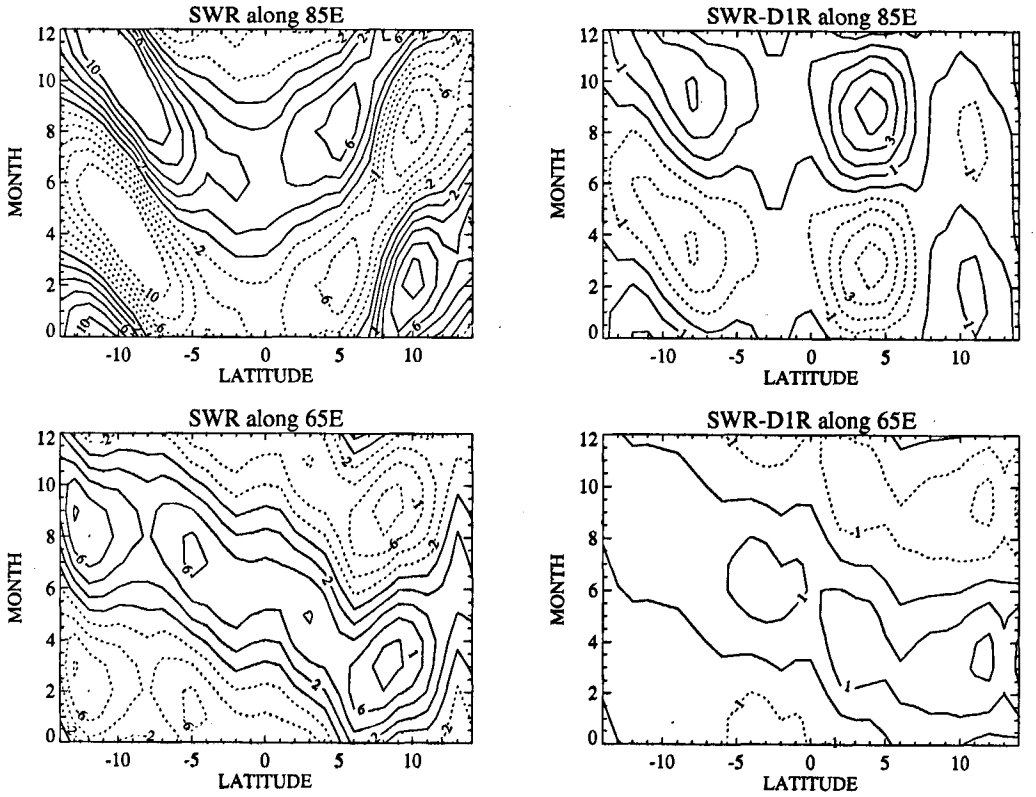

Figure 10

Meridional sections as a function of latitude and time of annual sea level variations from SWR and D1R. Same isocontour as Figures 4 e, f, g, h.

Sections méridiennes en fonction de la latitude et du temps des variations annuelles déduites de «SWR» et «D1R». Mêmes isocontours que sur la figure 4 *e, f, g, h.*

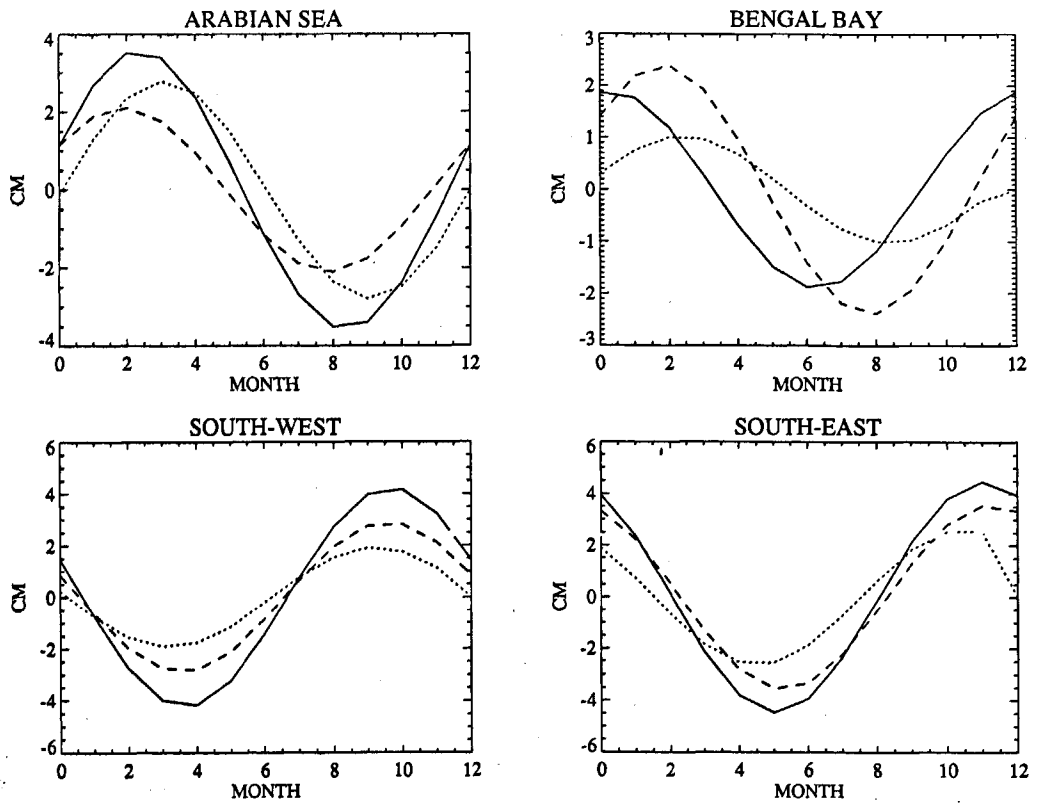

Figure 11

Basin averaged annual sea-level variations from SWR (plain), D1R (dashed) and model simulations (dotted) as a function of month (January is month 0 and 12). Basins are: Arabian Sea over 5°-25° N, 40°-75° E; Bay of Bengal over 80°-95° E, 5°-25° N; South-West over 40°-75° E, 20°-10° S; South-East over 80°-95° E, 20°-10° S.

Variations annuelles moyennées par bassin déduites de «SWR» (ligne pleine), «D1R» (tirets) et des simulations de modèle (pointillés) en fonction du mois de l'année (janvier est le mois 0 et 12). Les bassins sont : Mer d'Arabie = 5°-25°N, 40°-75°E ; baie du Bengale = 80°-95°E, 5°-25°N ; Sud-Ouest = 40°-75°E, 20°-10°S ; Sud-Est = 80°-95°E, 10°-20°S.

phase with the southern basin so that most of the satellite tracks have a large-scale along-track oceanic component. This is further evidenced on the basin-averaged variations (Fig. 11). In the Arabian Sea, SWR sea level drops by 7.5 cm from March to September while the southern basin rises by 8 cm (similar amplitude on the western and the eastern sides). Sea-level changes derived from D1R are only 4.7 and 5 cm respectively. In the Bay of Bengal, D1R sea level drops by 4 cm from March to September, actually more than the SWR drop (3 cm) which occurs two months earlier. When the averages over the northern are distinguished from those over southern basins, the difference increases by 19.6 cm between October and May for SWR and by 15.6 cm for D1R. For comparison, the variation differences between the same basins simulated by the model driven by FSU winds are overplotted. Note that the simulated north-south variations are of the same amplitude (15.0 cm) as the D1R and weaker than SWR. The variations driven by FSU winds being themselves stronger than those driven by ECMWF winds (12.0 cm), it is possible that SWR observes oceanic variations which are not wind-driven. This is under investigation.

Interranual variations show up in the contrast between the sea level averaged over different years. First, the sea level was averaged over twelve months (November 1987 to October 1988) and differenced with the previous twelve months in 1986-1987. Maps of this sea-level interannual change are very contrasted: the sea level is rising in the 20° tropical band and outside falling this band. The difference between the SWR and the D1R estimates is mostly a north-south tilt, so that the interannual sea-level changes are amplified in the southern and tropical bands and reduced north of 10° N: sea level rises by 2.9 cm or 1.3 cm when averaged over 50°-90° E and 10° S-10° N, and drops by 2.3 and 1.0 cm when averaged over 60°-100° E and 30°-10° S. Depending on the method, the estimates can thus be very different. Unfortunately, the signal gained by SWR *versus* D1R in this case was found to be polluted by the difference between FNOC and SSMI. In order to avoid this pollution, we then chose to differentiate periods after July 1987 when SSMI data became available. Figure 12 presents the 1988-minus-1987 difference of sea level when averaged over six months from July to December. The sea level changes are not as contrasted as in the previous case. Nonetheless, averaged over 50°-95° E and from the equator to 10° N, the sea-level rise is 3 cm for SWR *versus* 1 cm for D1R. In this case, the oceanic signal estimated by the SW method is three times larger than that estimated from the D1 method. Very little is at present known about the interannual sea-level fluctuations of the Indian Ocean. Simulations are very controversial because they are sensitive to the readjustment which takes place in the southernmost domain from 20° to 40° S. Observations derived from 54 months of Geosat data with a D1 method have been proposed as a "zeroth order" possibility (Périgaud and Delécluse, 1991 *a* and 1992). It would be worthwhile reprocessing the entire Geosat data set with improved orbit, tropospheric and ocean tide corrections.

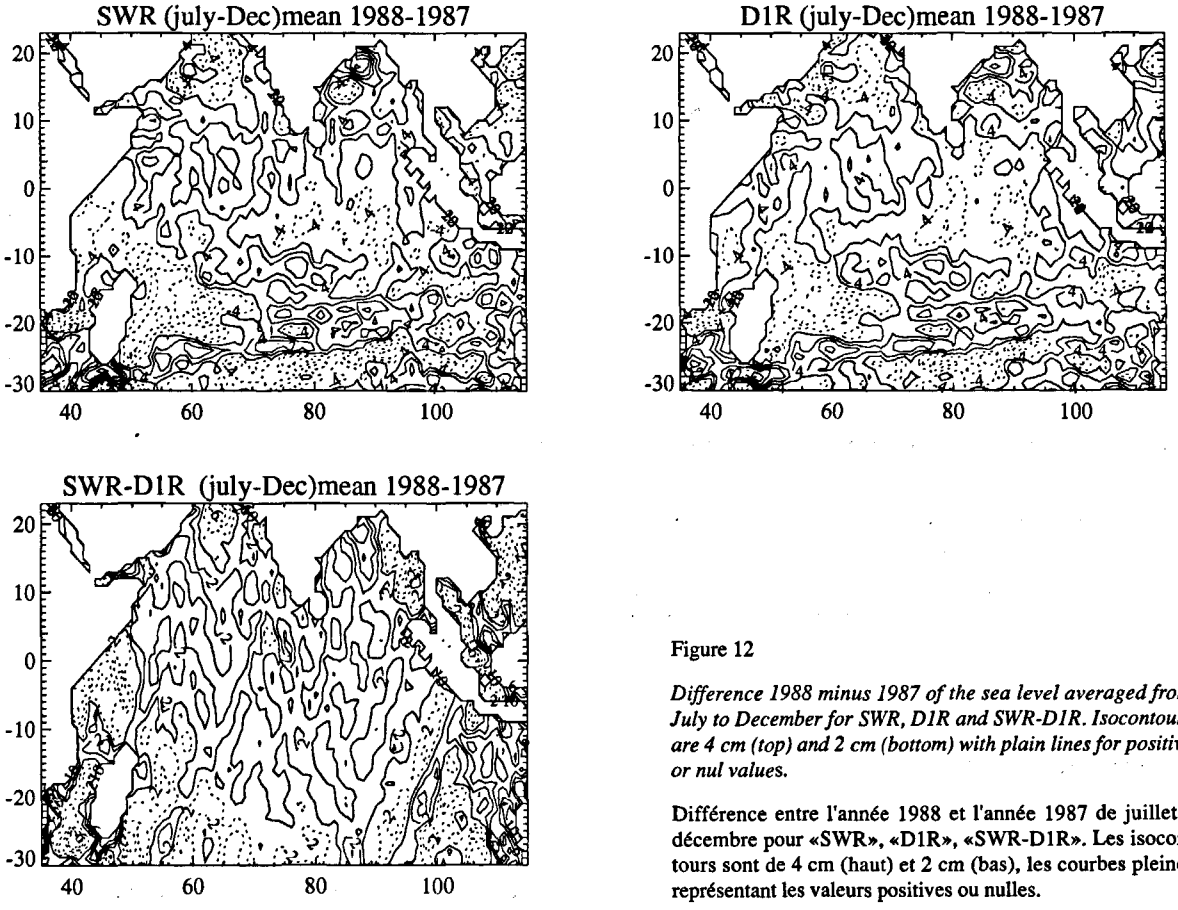

Figure 12

Difference 1988 minus 1987 of the sea level averaged from July to December for SWR, D1R and SWR-D1R. Isocontours are 4 cm (top) and 2 cm (bottom) with plain lines for positive or nul values.

Différence entre l'année 1988 et l'année 1987 de juillet à décembre pour «SWR», «D1R», «SWR-D1R». Les isocontours sont de 4 cm (haut) et 2 cm (bas), les courbes pleines représentant les valeurs positives ou nulles.

CONCLUSIONS AND DISCUSSION

We investigated how best to retrieve large-scale sea level changes within the Indian Ocean, especially possible interannual changes, from Geosat altimetric data. To this end, we compared two corrections for the residual orbit error, an along-track bias and trend over ~ 5000 km (labeled D1) and the sine of once per revolution (~ 40,000 km, labeled SW). We assessed the effect of residual M2 tidal errors, and removed much of their energy by applying a frequency-wavenumber filter that deletes those components with zonal wavelengths between 10.1° to 6.8° and periods between 395 to 263 days (the peculiar numbers result from the units of wavenumber and frequency, tied to the lengths of the space and time series).

Results with both orbit error schemes showed an error, with distinct space, time and propagation characteristics that match those of the M2 tide. Since the error propagates westward at about 3 km/day, it can be mistaken for Rossby waves at midlatitudes. Using the simulation described in the fourth section, the frequencies and wavenumbers aliased by the Geosat sampling were determined for the thirteen components used in the computation of the oceanic tide: except for S2, T2 and K2, all other components alias into wavelengths smaller than 10°.

While we are certain of the error identification, we cannot be sure of its origin: it could be due to uncertainty in the M2 coefficients in the Schwiderski's tidal model, or to a programming error (Cheney, 1989, pers. comm.; Le Provost, 1991, pers. comm.) known to have occurred in the production of the NOAA Geosat GDRs (Doyle *et al.*, 1989), which included the omission of the nodal coefficient correction and affected all the components of the oceanic tides. If the source is a coding error, then the new Geosat GDR being released on CD-ROM (Cheney, 1991, pers. comm.) should not show this effect; unfortunately, at the time of this study we only had access to the new data for part of 1987, so we performed a rather quick assessment of the difference between the tides in the old GDR and those in the new GDR. In the fifteen-day period between days 348 and 362 of 1986, the tidal corrections taken over the whole Earth differ by a mean of - 0.16 cm and an rms of 3.1 cm; extreme values of - 45 cm and 40 cm occur towards the end of this fortnight. In a box between longitudes 35° and 115° E and to the north of 30° S, roughly enclosing the Indian Ocean, the mean and rms differences are - 0.16 cm and 3.3 cm respectively, with extreme values of - 34 cm and 40 cm. Clearly these differences are important when assessing large scale, interannual changes in sea level.

After filtering out the tidal error [which contains about (2 cm)^2 variance], the SW residuals in the Indian Ocean have a variance of (9.5 cm)^2 with an annual component of (3.7 cm)^2, while the D1 residuals have a variance of (7.9 cm)^2 with an annual component of (3.0 cm)^2. The annual component, much stronger in the SW residuals, propagates westward and poleward as free Rossby waves (Schopf *et al.*, 1981). Such variations have been simulated with a shallow-water model driven by observed winds in the Indian Ocean over 1985-1989 (Périgaud and Delécluse, 1991 *b*). The interannual components (1988 average minus 1987 average, both for the months of July to December due to the availability of SSM/I water vapor) show the region between 50° and 95° E, Equator to 10° N, elevated in 1988; the rise is 3 cm with the SW residuals and 1 cm with the D1 residuals. These numbers are among the first estimates of interannual sea-level change in the Indian Ocean, so we have nothing to compare with; nor can we put a reliable formal error estimate on this result. The difference between D1 and SW calculations (2 cm) gives an idea of accuracy, but as we showed in the eighth section, the availability of FNOC *vs* SSM/I water vapor corrections also affects this result. Perhaps the simplest way to put it, is that we see a coherent interannual signal in the altimetrically derived sea level in the equatorial band of the Indian Ocean, a signal that deserves further attention.

The results presented in the foregoing sections confirm the common sense expectation that the SW orbit correction preserves the larger scales of the circulation better than the shorter D1 correction, but also preserves some errors in the altimetric system. Ideally, no residual orbit correction would be necessary if the error in the dynamic orbit computation which uses orbital dynamics, tracking data, and models of the various forces on the satellite (*e. g.*, Haines *et al.*, 1990) could be brought below the 10 cm mark. There is every reason to believe that the Topex/Poseidon mission, tracked with Doris, lasers and GPS will achieve that result after a few iterations on the orbit computation. Until then, ad-hoc residual orbit corrections, like the D1, SW, and better alternatives will be needed; but as the corrections become more focused, *i. e.*, they target residual orbit error better by modeling it more narrowly (*e. g.*, Denker and Rapp, 1990), other errors in the complex chain of corrections applied to the altimetric data will become important, as did the unexpected tidal error in our calculations.

Acknowledgements

The research described in this paper was carried out at the Jet Propulsion Laboratory, California Institute of Technology, under contract with the National Aeronautics and Space Administration.

APPENDIX

Sine-wave correction to residual orbit error

This Appendix summarizes the handling of the Geosat data and gives some details about the "sine-wave" orbit error adjustment.

1) We started with the GDR files released by NOAA in 1987 (Cheney *et al.*., 1987), applied the GDR-supplied corrections for Schwiderski tidal model, ionosphere and FNOC dry troposphere. The data were regridded to a uniform set of latitudes. A one-second record was presumed to

be a blunder and removed when: a) the land flag was set; b) the rms of the 1 second average exceeded 15 cm; c) sigma-0 exceeded 35 dB; and d) a despiking algorithm intended to identify 1-3 s wide spikes flagged the record (Zlotnicki *et al.*, 1990). We then applied the FNOC wet tropospheric correction up to 7/87, and the Wentz (1989) wet tropospheric correction from DMSP-8 SSM/I data between 7/87 and 12/88. We applied an inverse barometer correction using the FNOC sea surface pressure implied by the FNOC dry tropospheric correction field of the GDR.

2) A "rev" was defined as the set of data starting at the highest latitude achievable by the satellite, and ending one period (~ 101 minutes) later.

A "nest" was defined as the set of revs (usually 45, every 17.0505 days) with the same groundtrack, covering the time 8/11/86 to 12/31/88.

3) For each nest, indexed by "k", and each rev, indexed by "j", the along-track altimeter heights, indexed by "i" along the most complete rev, "j_0" were removed from all revs in the nest, yielding height differences:

$$\delta h_{ijj_0k} = h_{ijk} - h_{ij_0k} \qquad \text{(A1)}$$

Then, the following function was fit by simple least squares to the dhijj0k to estimate orbit error:

$$e_h = A_{jj_0k} + B_{jj_0k}.\sin(\omega t) + C_{jj_0k}.\cos(\omega t), \qquad \text{(A2)}$$

$$\text{with } \omega = 2\pi/T, \quad t_2(j,k) \le t \le t_0(j,k) + T,$$

$$T = 6031.51 \text{ s} \qquad \text{(A3)}$$

(notice that both the height differences and the A,B,C coefficients for rev j_0 are zero).

4) The average coefficients over all revs of a nest were then removed from the coefficients of each rev in the same nest, equivalent to a statement that the average orbit error along that groundtrack over two years is zero. In symbols,

$$C_{jk} = C_{jj_0k} - (1/jmax) \sum_{j'=1}^{jmax} C_{j'j_0k} \qquad \text{(A4)}$$

and similarly with the B and A coefficients. This approach is essentially similar to the more straightforward approach based on averaging the heights first, but allows for better handling of data gaps.

Over most of 1987 the error amplitudes $\sqrt{B^2+C^2}$ were lower than for 1988; the error is worst in the second half of 1988. The rms amplitudes (errors) are 17.0 cm in 1986-1987, 40.1 cm in 1988, and 30.1 cm over the whole 25.6 months. The second half of 1988 is associated with much increased solar activity, which affects the heights in two ways: a) it increases the non-conservative radiation pressure on the satellite and makes its accurate modeling in the programs that integrate the orbital equations more difficult; b) it affects the accuracy of the ionospheric correction applied to the altimeter. However, the second effect is only of the order of 1-5 cm (*see* Musman *et al.*, 1990) so it is the first effect that causes the increased orbit error.

REFERENCES

Arnault S., Y. Ménard and J. Merle (1990). Observing the tropical Atlantic Ocean in 1986-1987 from altimetry. *J. geophys. Res.*, **95**, 17921-17945.

Cartwright D.E. and R.D. Ray (1990). Oceanic tides from Geosat Altimetry. *J. geophys. Res.*, **95**, 3069-3090.

Cartwright D.E., R.D. Ray and B.V. Sanchez (1991). Oceanic Tide Maps and Spherical Harmonic Coefficients from Geosat Altimetry. NASA Tech. Memorandum 104544, 1-74.

Cheney R.E., B.C. Douglas, R.W. Agreen, L.L. Miller and D.L. Porter (1987). Geosat Altimeter geophysical Data record (GDR) User Handbook. NOAA Tech. Mem. NOS NGS-46, Rockville, MD, 32 pp.

Denker H. and R. Rapp (1990). Geodetic and Oceanographic results from the analysis of 1 year of Geosat data. *J. geophys. Res.*, **95**, c8, 13151-13168.

Doyle N.S., B.C. Cheney, B.C. Douglas, R.W. Agreen, L. Miller and E.L. Timmerman (1989). The NOAA Geosat GDR 's: summary of the second year of the exact repeat mission. NOAA Tech. Mem., NOS NGS-49.

Haines B.J., G.H. Born, G.W. Rosborough and J.G. Marsh (1990). Precise Geosat Orbits for the Geosat Exact Repeat Mission. *J. geophys. Res.*, **95**, C3, 2857-2870.

Jacobs G.A., G.H. Born and P.C. Allen (1991). The global structure of the annual and semi-annual sea surface height variability from Geosat altimeter data. submitted to *J. geophys. Res.*

Mazzegga P. (1985). M2 model of the global ocean tide derived from Seasat Altimetry. *Mar. Geod.*, **9**, 335-363.

Miller L., R.E. Cheney and B.C. Douglas (1988). Geosat altimeter observations of Kelvin waves and the 1986-1987 El Niño. *Science*, **239**, 52-54.

Musman S., A. Drew and B. Douglas (1990). Ionospheric effects on Geosat altimeter observations. *J. geophys. Res.*, **95**, C3, 2965-2968.

Périgaud C. (1990). Sea-level oscillations observed with Geosat along the two shear fronts of the Pacific North equatorial Countercurrent. *J. geophys. Res.*, **95**, 7239-7248.

Périgaud C. and P. Delécluse (1989). Simulations of dynamic topography in the Northwestern Indian Ocean with input of Seasat altimeter and scatterometer data. *Ocean-air Interactions*, **1**, 289-309.

Périgaud C. and P. Delécluse (1991 *a*). Observed and simulated low-frequency sea level variations in the tropical Indian Ocean. *Proceedings of the URI Theoretical Equatorial Panel Meeting*, J. McCreary and D. Moore, editors, in press.

Périgaud C. and P. Delécluse (1991 *b*). Annual sea-level variations in the Southeastern tropical Indian Ocean. *J. geophys. Res.* (in press).

Périgaud C. and P. Delécluse (1992). *Low-Frequency sea level variations in the Indian Ocean from Geosat altimeter and shallow-water simulations. Research Trends in Oceanography*, CSRI Ed., Trivandrum, India, in press.

Périgaud C. and V. Zlotnicki (1992). Error analysis on annual sea-level variations in the tropical Indian Ocean derived from Geosat and shallow-water simulations, to be submitted to *J. geophys. Res.*

Rao R.R., R.L. Molinari and J.F. Festa (1989). Evolution of Climatological Near-Surface Thermal Structure of the tropical Indian Ocean. 1) Description of Mean Monthly Mixed Layer Depth, and Sea Surface Temperature, Surface Current, and Surface Meteorological Fields. *J. geophys. Res.*, **94**, 10801-10815.

Sandwell D.T. and B. Zhang (1989). Global mesoscale variability from the Geosat Exact Repeat Mission: Correlation with Ocean Depth. *J. geophys. Res.*, **94**, 17971-17984.

Schopf P., D. Anderson and R.Smith (1981). Beta dispersion of low-frequency Rossby waves. *Dynam. Atmos. Oceans*, **5**, 187-214.

Schott F. (1987). *Recent studies of western Indian Ocean circulation. Further Progress in Equatorial Oceanography*, Nova University Press, E. Katz and J. Witte, editors. 287-302.

Tai C.-K. (1991). How to observe the gyre to global scale variability in satellite altimetry: signal attenuation by orbit error removal, *J. atmos. ocean. Technol.*, **8**, 271-288.

Wentz F.J. (1988). Water vapor length correction for altimeters. USA WOCE Tech. Rept 2, US Planning Office for WOCE, College Station, TX (available from Appendix).

Wentz F.J. (1989). User's Manual SSM/I Geophysical Tapes. RSS Tech. Report 060989, Remote Sensing Systems, Santa Rosa, CA, 16 pp.

Wyrtki K. (1971). Oceanographic Atlas of the International Indian Ocean Expedition, in: *Dynamic topography and Mass transport.* NSF Washington, 359-394.

Zlotnicki V. (1991). Sea-level differences across the Gulf Stream and Kuroshio extension. *J. phys. Oceanogr.*, **21**, 4, 599-609.

Zlotnicki V., L.-L. Fu and W. Patzert (1989). Seasonal Variability in Global Sea Level observed with Geosat altimetry. *J. geophys. Res.*, **94**, C12, 17959-17970.

Zlotnicki V., A. Hayashi and L.L. Fu (1990). The JPL-Oceans-9802 version of Geosat Altimetry data. internal document JPL, D-6939, 17 pp.